JOURNAL OF MATERIALS SCIENCE 25 (1990) 2004–2010

Plastic behaviour under simple shear of thermosetting resins for fibre composite matrices

C. G'SELL
Laboratoire de Physique du Solide (URA D0838) Ecole des Mines, Parc de Saurupt, 54042 Nancy-Cedex, France

D. JACQUES, J. P. FAVRE
ONERA, Département Matériaux, 92322 Chatillon-Cedex, France

Simple shear tests have been performed on four different types of resins (cyanate and epoxy-based) which are usually employed for carbon composites. Unexpectedly, all the resins exhibited an intensive plastic response, even at room temperature. Most of the specimens could undergo, at least in their central part, a local shear strain as large as about 0.5. Their constitutive behaviour is very similar to those of glassy thermoplastics – visco-elastic stage, strain softening, shear banding, strain hardening, ultimately homogeneous strain and rupture. It appeared that τ_y decreases with T_g. The results are discussed in terms of the molecular mechanisms of plasticity. Some consequences on the micromechanics of fibre-reinforced composites are also presented.

1. Introduction

In fibre reinforced composites with thermosetting resin matrices, the ultimate strength is more often controlled by shear fracture mechanisms, either at the interface between two plies (delamination), or at the interface between the fibres and the polymeric matrix [1–4].

It is then important to analyse separately the intrinsic failure mechanisms of the matrix, and the effects associated with the presence of the fibres. In this paper, the interest will be focused on the former aspect of the problem, with a particular attention paid to the yielding of commonly used industrial resins.

Although the elastic or visco-elastic properties of a variety of matrices are regularly published [e.g. 5], little is known about their plastic response. Only a few data have been reported hitherto on the yield behaviour of thermosets in uniaxial compression [6–10], and hardly any under shear, because the common shear tests (torsion, rail shear, short beam flexion, plane strain compression) are usually very tedious to perform, or difficult to analyse. Thanks to a novel testing procedure in simple shear with automated computer control, the plastic constitutive equation of several resins was determined in this work up to relatively large amounts of plastic strain. The results will be presented and then discussed in terms of recent theories concerning the plastic deformation mechanisms of glassy polymers.

2. Experimental techniques

2.1. Materials selection

Four types of thermosetting resins were experimented (noted *A* to *D* in Table I). The first one is based on a Bisphenol-A polycyanate, the others are of the epoxy type. All the materials were subjected to the same curing conditions (2 h at 180° C). Only for one of them (*D*), a number of extra samples (*D*2) were cured with a special 2-step schedule (1 hour at 175° C followed by 4 h at 190° C). The glass transition temperature of the materials (T_g) was determined by means of a torsion pendulum with special

TABLE I Characteristics of the resins investigated

Ref	Industrial reference	Chemical Nature	Curing schedule	T_g (° C)
A	NARMCO 5245	cyanate-base	2 h at 180° C	247.5
B	NARMCO 5208	TGMDA/DDS	2 h at 180° C	264
C	CIBA 6376	TGMDA/DDA	2 h at 180° C	250
D1	CIBA 914	TGMDA/DDA	2 h at 180° C	180
D2	CIBA 914	TGMDA/DDA	1 h at 175° C +4 h at 190° C	228

0022–2461/90 $03.00 + .12

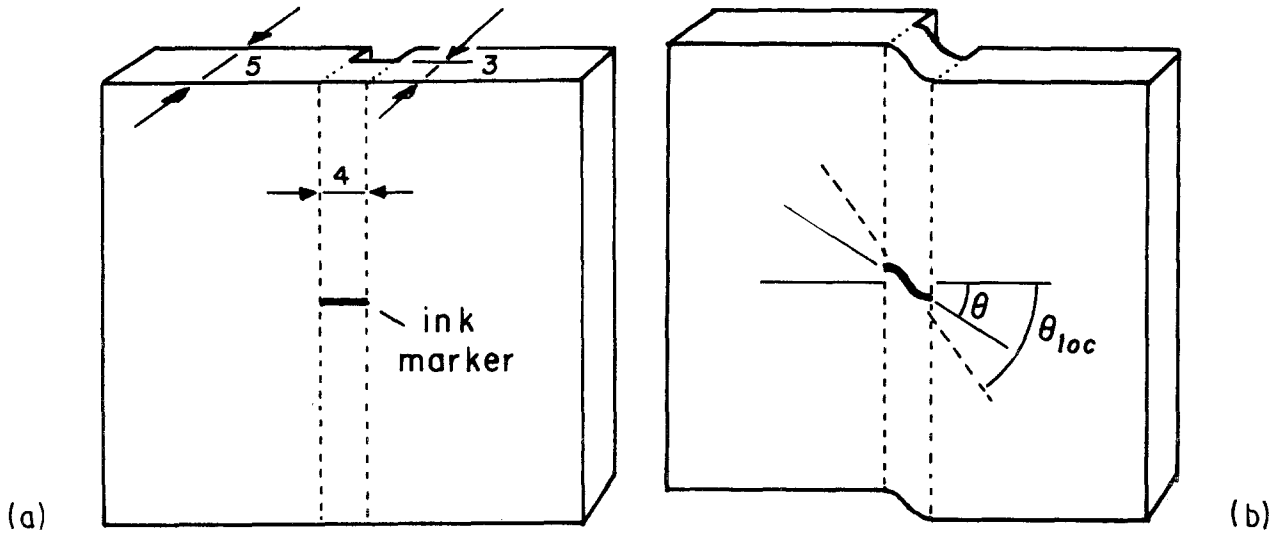

Figure 1 Geometry of a simple shear specimen (a) before the test, (b) during the deformation process.

parallelepipedic specimens cut out of the moulded resins [11]. The glass transition temperature was obtained from the maximum damping temperature.

2.2. Simple shear testing method

A special shear test has been developed by one of the authors (*C. G'.*) and previously applied to the investigation of the plastic behaviour of various thermoplastic polymers [12, 13] and sheet metals [14]. The shape of the testpieces is illustrated in Fig. 1a. The central calibrated portion (delimitated by the longitudinal groove) is characterized by the following dimensions, width $h = 4\,\text{mm}$, thickness $e = 3\,\text{mm}$, length $L = 60\,\text{mm}$. The massive heads on both sides are designed to attach the sample in the grips of the shearing apparatus. One face of the specimens is flat polished and printed with a flexible serigraphic ink marker in order to characterize the local distortion of the material in the centre of the calibrated part.

The shearing stage is mainly similar to previously developed "rail shear" systems [15–16], insofar as the heads are displaced parallel to each other with no variation of the width, h, of the calibrated part. The overall strain field is thus of the simple shear type and characterized by the applied shear $\gamma = x/h$, where x is the relative displacement of the heads, and the applied shear stress $\tau = F/(L.e)$, where F is the applied force. The novel aspects of the technique employed here is that the shear stage, (i) is very compact and adaptable to conventional tensile machines, (ii) the dimensions of the specimens are optimized for precise measurement of strain and stress with a close respect of the simple shear boundary conditions [12] and (iii) the strain distribution across the calibrated part is monitored in real time during the shear test by a computer interfaced video camera which records the actual shape of the ink marker. The latter point in the list above has been proved to be important in the case of polymeric materials [17]. It was stated indeed, that shear strain gradients are likely to develop in a resin if the stress–strain curve presents a softening stage. Recording the marker shape printed on the specimen surface allows one to measure the local shear $\gamma_{loc} = tg\ \theta_{loc}$ from the local inclination of the ink marker (Fig. 1b), the mean inclination of the marker, θ, giving access to the overall (applied) shear: $\gamma = tg\ \theta$. The complete experimental set up is schematized in Fig. 2. In all the experiments reported below, the applied

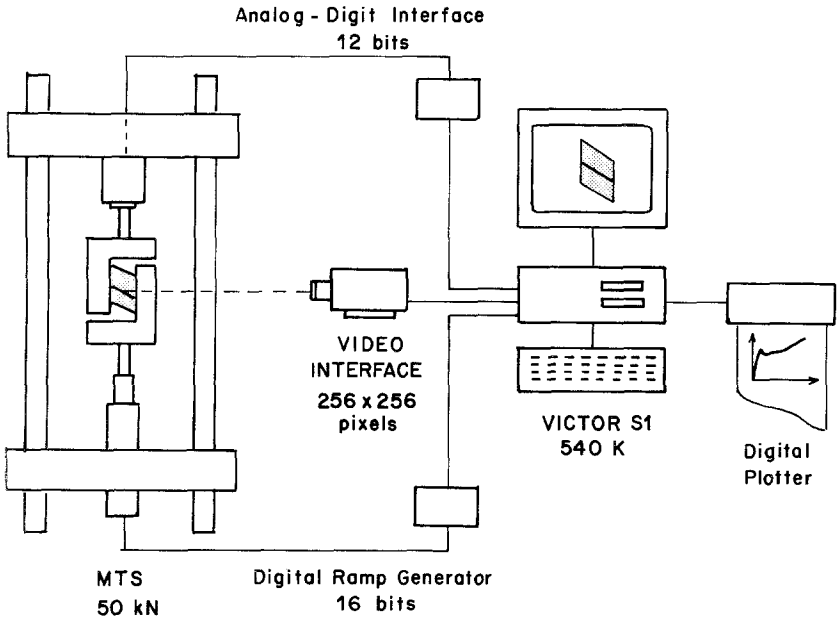

Figure 2 General diagram of the simple shear system. Notice the computer aided video shear transducer.

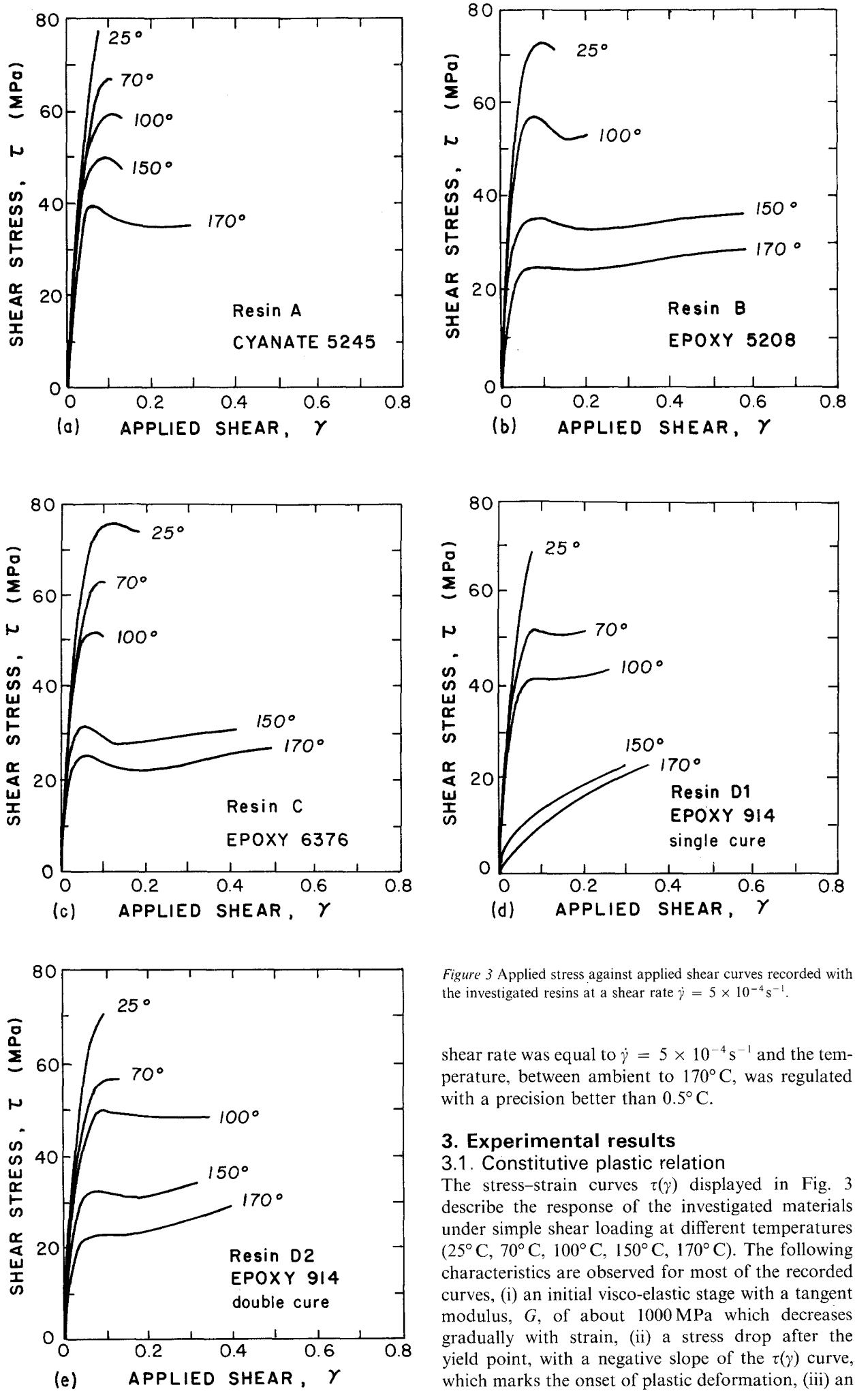

Figure 3 Applied stress against applied shear curves recorded with the investigated resins at a shear rate $\dot{\gamma} = 5 \times 10^{-4} s^{-1}$.

shear rate was equal to $\dot{\gamma} = 5 \times 10^{-4} s^{-1}$ and the temperature, between ambient to 170° C, was regulated with a precision better than 0.5° C.

3. Experimental results

3.1. Constitutive plastic relation

The stress–strain curves $\tau(\gamma)$ displayed in Fig. 3 describe the response of the investigated materials under simple shear loading at different temperatures (25° C, 70° C, 100° C, 150° C, 170° C). The following characteristics are observed for most of the recorded curves, (i) an initial visco-elastic stage with a tangent modulus, G, of about 1000 MPa which decreases gradually with strain, (ii) a stress drop after the yield point, with a negative slope of the $\tau(\gamma)$ curve, which marks the onset of plastic deformation, (iii) an

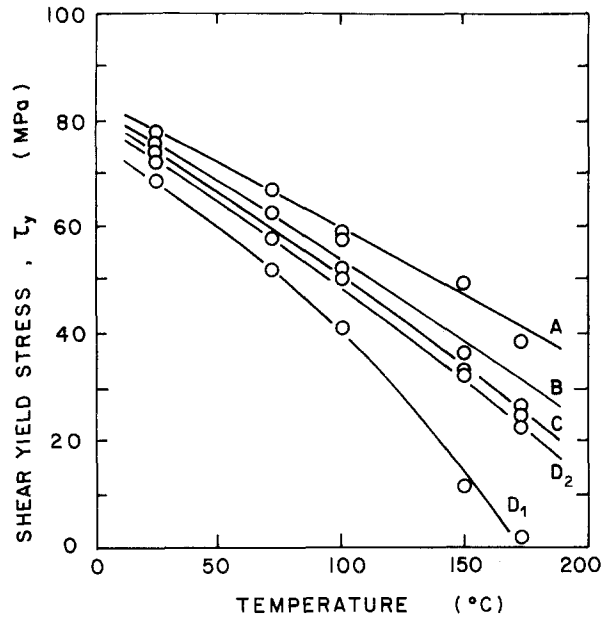

Figure 4 Influence of temperature on the shear yield stress for the resins investigated.

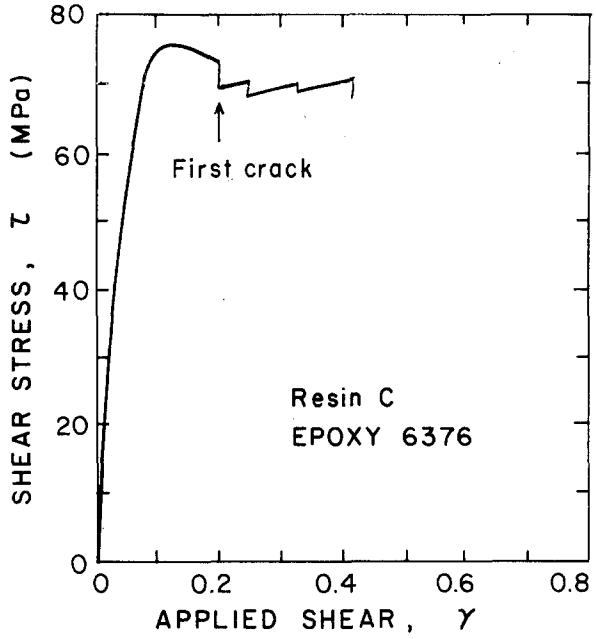

Figure 5 Example of the shear behaviour past the formation of the first crack (resin *C*).

ultimate plastic stage with a moderately positive strain hardening rate.

However, for some of the tested samples, the $\tau(\gamma)$ curve differs from the typical pattern reported above; some of them broke at the end of the visco-elastic stage with no visible plastic yielding (e.g. resin *A* at 25° C), others deformed extensively without any definite visco-elastic stage (e.g. resin *D*1 at 150° C and 170° C).

The influence of temperature on the yield stress τ_y of the materials tested is illustrated in Fig. 4. The following conventions were adopted for the determination of these data, (i) when the $\tau(\gamma)$ curve presented a softening stage τ_y was taken at the upper yield point, (ii) when the sample fractured at the end of the viscoelastic stage, τ_y was taken as the fracture stress and, (iii) when the curve showed a monotonous rise without softening effect, τ_y was obtained at the intersect of the extrapolated viscoelastic and plastic stages. It is evident that the yield stress decreases regularly with temperature. It should be noticed in particular that the value of τ_y at 25° C can be obtained by a simple extrapolation of the data at higher temperatures. The latter result indicates that the material failure at 25° C is controlled by plastic micromechanisms in all cases, and not by simple cleavage in spite of the aspect of the $\tau(\gamma)$ curves, which could have been interpreted as representative of a brittle material. The tested resins are classified in decreasing order of τ_y following, *A*, *B*, *C*, *D*2, *D*1. The particular behaviour of the materials *D*1 at 150° C and 170° C is justified by the very low T_g of this resin (180° C). Also in the torsion pendulum experiments, the apparent torsion modulus began to depress considerably at temperatures below the maximum damping transition. The recorded curves in these particular shear tests are then representative of an intermediate behaviour between easy plastic and rubber-like ones.

3.2. Rupture strain

The shear deformation of the samples was limited by the development of one or several cracks at the upper and lower ends of the calibrated part, long before the central zone (where shear strain is measured) was damaged. In the curves of Fig. 3, we have plotted the $\tau(\gamma)$ data up to the point when the first crack was recorded. Nevertheless, the tests were continued beyond this first damage. As an example of the ultimate behaviour, the complete $\tau(\gamma)$ curve for the resin *C* at 25° C is displayed in Fig. 5. It should be noticed that the shear strain ultimately attained in the centre of the sample is as large as 0.4 while the "rupture strain" corresponding to the first recorded crack is 0.2 only. We have shown elsewhere [13], that the preferential formation of cracks at the ends of a simple shear testpiece is due to the perturbation introduced in the otherwise plane deformation field by the local presence of the free end surface. We have declined to plot the ultimate portion of the $\tau(\gamma)$ curves in Fig. 3 since, although the recorded γ data are correct, the corresponding τ values lose their intrinsic signification as soon as cracks begin to form at the sample extremities (the effective cross-section is then reduced by an unpredictable ratio).

Furthermore, it was demonstrated several times in various polymers that the onset of cracking is strongly influenced by the presence of microscopic imperfections (microcracks, crazes, scratches . . .). Consequently, it seems clear that the failure onset strain should not be considered as a precise measurement of the deformability for a given resin since a material element situated far from the sample boundaries can undergo much larger shear strains without damage.

One should then recall from these experiments that all the thermosets tested here have a *potential* ability to deform plastically under simple shear, even at room temperature. However, this plastic behaviour competes with a *concurrent* rupture mechanism which is earlier as the temperature is lower and the local stress tensor has a larger dilatant hydrostatic component [18].

3.3. Development of strain gradients

It has been proved previously [13, 19] that the plastic deformation of glassy polymers is stable only when the shear stress increases with strain (positive strain hardening). By contrast, the deformation tends to localize as soon as the material strain-softens ($d\tau/d\gamma < 0$) and this localization is faster as the strain hardening is more negative. For the resins studied in this work, we have reported in a preceding section that their $\tau(\gamma)$ curve exhibits, in most cases, a negative slope stage. Deformation instability should then be expected through the occurrence of *shear bands*. As an illustrating case, let us examine the epoxy resin *C* tested at 170° C. The $\tau(\gamma)$ curve (Fig. 3) shows a marked yield point at 25 MPa, followed by a moderate but clear softening stage up to an applied shear strain of 0.2. Beyond this point, the slope is positive again. The computer-assisted video system has recorded during the test the evolution of the ink marker distortions which was originally straight and horizontal (Fig. 6). Homogeneous deformation would have been correlated to a simple rotation of the marker. Actually, it is evident that it takes a sigmoidal shape with a maximum local shear in the median part of the calibrated portion. As an example, for $\gamma = 0.2$, the maximum shear is $\gamma_{loc} = 0.4$. This strain distribution, observed along the whole specimen, corresponds to a unique, 60 mm long shear band. It is noticed that the lateral limits of this band are not marked by an abrupt shear discontinuity, but rather by a gradual transition over a width of about 500 μm. The band is observed to be formed at the upper yield point. Its maximum shear grows rapidly during the softening period. Afterwards, as the material resumes its hardening, the band tends to widen as its maximum shear continues to increase slowly (Fig. 6). The record obtained at $\gamma = 0.6$ shows that the band has invaded the whole calibrated portion, i.e. the deformation has then recovered its homogeneity and γ_{loc} is uniformly equal to γ.

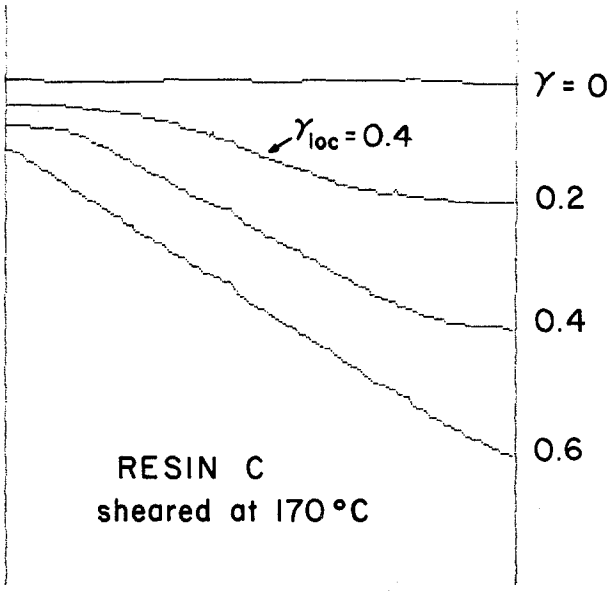

Figure 6 Gradual distorsion of the printed ink marker during the shear test for the resin *C* at 170° C.

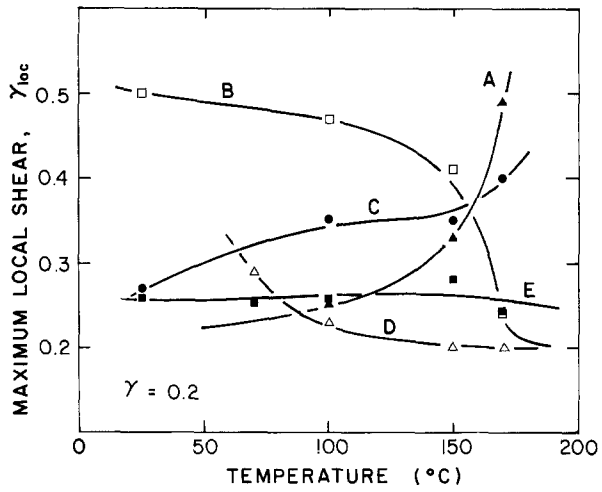

Figure 7 Influence of temperature on the maximum local shear γ_{loc} in the shear band at $\gamma = 0.2$.

It would be useful to study with closer details the kinetics of shear band formation during the softening stage. This point will be studied in a later development of the work. However, we are presently able to conclude that considerable local shear strains can be recorded in the shear bands of thermosetting resins, even for a rather moderate overall shear, just past the visco-elastic limit. Quantitatively, Fig. 7 gives the maximum local shear at the centre of the shear band for tests performed at all temperatures and for an applied shear of 0.2. Although the various tendencies illustrated by this plot for the different resins cannot be readily interpreted, it is evident that the stronger materials (*A*, *B*, *C*) exhibit the highest tendency to strain localization in a given temperature range, since the local shear strain in the band may be as high as 2.5 times the overall strain.

4. Discussion

In contrast with their brittle tensile behaviour, the polymeric composite matrices experimented in this work exhibit an extensive plastic response under simple shear, even at room temperature. Furthermore, it should be remarked that their cross-linked macromolecular structure does not seem to make this plastic behaviour very different to those of glassy thermoplastic polymers under the same loading conditions. As an example of this statement, the corresponding $\tau(\gamma)$ curves of amorphous polycarbonate are displayed in Fig. 8 at different temperatures. It is evident that the same features are found with, (i) a strain softening stage followed by strain hardening, (ii) the development of a unique shear band, and (iii) the gradual decrease of τ_y with temperature. The main difference which can be noticed is the very large shear strain which can be undergone by the linear polycarbonate at rupture while the cross-linked resins survived to shear strains of about $\gamma = 0.5$ only.

This close similarity between thermosets and thermoplastics in their ability to undergo plastic yielding leads to several consequences, as well on a fundamental point of view as in practical applications.

In previous papers, a number of authors have already acknowledged the plastic flow ability of cross-

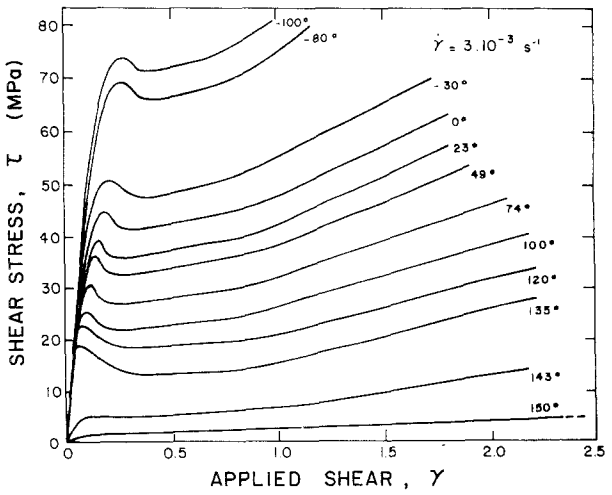

Figure 8 Plastic behaviour of amorphous polycarbonate under simple shear at various temperatures.

linked resins, especially in uniaxial or plane strain compression, and in the range of preplastic strains or just past the yield point. For example, some experimental data were presented and discussed on cured resins such as epoxies [6, 20], polyimides [7, 8], unsaturated polyesters [9], polyurethanes [10], and others. It results from these studies that the plastic deformation of strongly cross-linked resins proceeds, as for linear thermoplastics below T_g, by the activation of very local macromolecular mechanisms. Under the effect of thermal agitation and applied stresses, elementary molecular jumps occur, in order to accommodate the imposed deformation against the interaction of the closest molecular groups situated in the same chain (intra-molecular interactions) or in the neighbouring chains (inter-molecular interactions). A sufficient chain mobility is allowed by the movement of very short molecular segments including a few simple covalent bonds [21], so that the presence of cross-links does not impede too seriously the local mobility of polymeric chains, at least in the range of moderate strains. It is important to note that whatever can be the type of loading applied to the material, macromolecular plasticity always proceeds by shear mechanisms which minimize material diffusion and volume changes. Several theories have been proposed to predict the influence of various parameters (temperature, strain rate, molecular structure . . .) on the plastic behaviour of polymeric glasses. Although they are based on different elementary mechanisms, like disclinations [22], dislocations loops [23] or microshear domains [17], they have important common features as (i) the strong influence of the macroscopic elastic modulus on the molecular jumps [24], (ii) the small characteristic size of the basic deformation element, whose dimensions are of the order of 0.4 mm, (iii) the cooperative activation of plastic events in neighbouring elements leading to strain softening and shear banding and, (iv) the gradual orientation of polymeric chains under local shear, leading to the ultimate strain-hardening of the material. The particular aspects of thermosetting resins in this scope come from the limitation of the molecular freedom imposed by the relative intrinsic rigidity of the chains and by the presence of cross-links. These constraints lead to relatively higher yield stresses and to smaller rupture strains than in many thermoplastic polymers.

In addition to the above properties, the resins tested in the present study show the following behaviour. It is observed that their respective plastic response presents some correlation with their glass transition temperature. It is evident, indeed, that those resins whose T_g is higher, have also the highest yield stress. This final point supports the dependence of plastic yielding on local mobility mechanisms of the same type as those activated in a more collective way at glass transition [25].

Among the industrial applications of thermosets, the most leading ones are the load-transmitting matrices in the high performance fibre reinforced composites. Although the large elastic modulus of composites is mostly controlled by the rigidity of the fibres, several aspects of the micromechanics as well as the macromechanics of the laminates depend on the constitutive equation of the matrix (26).

Whatever the type of stress or damage, it is now agreed that the resin properties are always to be taken into account. As far as crack propagation is concerned, for example, the delamination resistance of the unidirectional composite has been shown to be clearly promoted by the ability of the matrix to withstand plastic deformation [2] – the recent high toughness composites have actually taken great advantage of the enhanced ductility of the crystallized thermoplastic matrix.

Concerning more diffuse damage processes, it is now clear that the ultimate properties of the unidirectional composite are not only dependent on the fibre resistance but also on the plastic law of the organic matrix. Even for tension in the direction parallel to the fibres, where the role of the matrix is rather secondary, the statistical process of progressive fibre breaking is deeply controlled by the reloading capability of the matrix at the fibre ends. Various contributions have put the emphasis on the stress state supported by the resin close to the tip of broken fibres, ultimately resolving either by plastic deformation, or by some cracking or debonding [27–29]. For any other direction, the plastic capability of the matrix assumes far more importance. In longitudinal compression, for example, the matrix is subjected to simple shear as soon as the fibres begin to buckle, resulting in a gradual increase of the ultimate compressive properties with the shear strength of the resin [1]. Also in the still ambiguous transverse direction, the composite strength is raised above the matrix strength, or is smaller than it according to the more or less pronounced ductility of the resin, due to the high stress concentration at the fibre/matrix interface and the biaxial state of stress in the resin [30].

For practical angle-ply composites, the resin properties are also expected to influence the overall laminate behaviour even if the stress state often defeats the simple analysis.

5. Conclusions

Four different thermosets (cyanate and epoxy-based

resins) were subjected to simple shear testing with a special shearing device which allows to record the $\tau(\gamma)$ curve and the evolution of the local strain distribution, simultaneously. The following conclusions can be drawn from these experiments: (1) All the resins exhibit a pronounced plastic behaviour, even at room temperature. (2) Shear strains as large as 0.5 can often be attained in the centre of the specimen, even though failure begins at its ends at an earlier moment. (3) An early plastic instability phenomenon occurs at the yield point under the form of a unique shear band. It grows during the whole softening stage before stabilizing when hardening resumes. (4) Many similarities are observed between the behaviour of these thermosets and the plasticity of glassy thermoplastics, although those exhibit a larger ultimate strain. This observation promotes plasticity mechanisms involving very local elementary chain movements.

The above results serve as important ingredients for the interpretation of the failure mechanisms in resin-based fibre-reinforced composites. They show in particular that any rupture model founded solely on the elastic deformation of the matrix would underestimate the capability of the thermosets to relax the local stress concentrations in the material by the extensive accommodation of localized strains at the fibre-matrix interface and at the interface between crossed plies.

References

1. S. W. TSAI and H. T. HAHN, "Introduction to Composite Materials", (Technomic, Westport 1980) p. 414.
2. W. L. BRADLEY and R. N. COHEN, in "Delamination and Debonding of Materials", W. S. Johnson Ed., (ASTM STP 876, Philadelphia 1985) p. 389.
3. K. W. GARRETT and J. E. BAILEY, *J. Mater. Sci.* **12** (1977) 2189.
4. J. E. BAILEY and A. PARVIZI, *J. Mater. Sci.* **16** (1981) 649.
5. N. HATA and J. KUMANOTANI, *J. Appl. Polym. Sci.* **15** (1971) 2371.
6. S. YAMINI and R. J. YOUNG, *J. Mater. Sci.* **15** (1980) 1814.
7. A. S. ARGON and M. J. BESSONOV, *Polymer Engng. Sci.*, **17** (1977) 174.
8. J. M. LEFEBVRE, C. BULTEL and B. ESCAIG, *J. Mater. Sci.* **19** (1984) 2415.
9. G. COULON, J. M. LEFEBVRE and B. ESCAIG, *Polym. Bull.* **12** (1984) 399.
10. Y. LETERRIER and C. G'SELL, *J. Mater. Sci.* **23** (1989) 4209.
11. D. BOUVART, J. P. FAVRE, J. C. MATRAN and M. C. MERIENNE, Proceedings 1st European Conference on Composite Materials (Bordeaux, France 1985) p. 322.
12. C. G'SELL, S. BONI and S. SHRIVASTAVA, *J. Mater. Sci.* **18** (1983) 903.
13. C. G'SELL and A. J. GOPEZ, *J. Mater. Sci.* **20** (1985) 3462.
14. E. RAUCH and C. G'SELL, *Mat. Sci. Engng.* **A111** (1989) 71.
15. J. M. WHITNEY, D. L. STANSBARGER and H. B. HOWELL, *J. Compos. Mater.* **5** (1971) 24.
16. R. CARCIA, T. A. WEISSHAAR and R. R. McWHITHEY, *Exper. Mech.* August (1980) 273.
17. C. G'SELL, in "Strength of Metals and Alloys", Edited by H. J. McQueen *et al.* (Pergamon Press, Oxford, UK, 1986) **Vol. 3**, p. 1946.
18. S. S. STERNSTEIN, in "Polymeric Materials", (American Society for Metals, Metals Park, Ohio 1975) p. 369.
19. C. G'SELL, *Rev. Phys. Appl.* **23** (1988) 1085.
20. P. B. BOWDEN and J. A. JUKES, *J. Mater. Sci.* **7** (1972) 52.
21. I. V. YANNAS and R. R. LUISE, in "The Strength and Stiffness of Polymers" Edited by A. E. Zachariades and R. S. Porter, (Dekker, New York 1983) p. 255.
22. A. S. ARGON, *Phil. Mag.* **28** (1973) 839.
23. P. B. BOWDEN and S. RAHA, *Phil. Mag.* **29** (1974) 149.
24. M. KITAGAWA, *J. Polym. Sci.* Polymer Phys. Edn. **15** (1977) 1601.
25. C. BAUWENS-CROWET, J. C. BAUWENS and G. HOMES, *J. Mater. Sci.* **7** (1972) 176.
26. M. R. PIGGOTT, in "Failure of Plastics", Edited by W. Brostow and R. D. Corneliussen, (Hanser, Munich 1986) p. 443.
27. J. O. OUTWATER Jr., *Mod. Plast.* **33** (1956) 156.
28. M. G. BADER, *Sci. and Engng. of Compos. Mater.* **1** (1989) 1.
29. D. JACQUES, Thèse de Doctorat, (I.N.P.L., Nancy, France 1988).
30. D. J. NICHOLLS, in "Composite Materials Testing and Design", Edited by J. M. Whitney, (ASTM STP 893, Philadelphia 1984) p. 109.

Received 3 January
and accepted 17 July 1989